Influence of Porosity in the Fatigue Behaviour of the High Pressure Die Casting AZ91 Magnesium Alloys

M. Preciado[1], P. M. Bravo[1], D. Cárdenas[1]

[1] University of Burgos. Avda. Cantabria s/n. 09006 Burgos, Spain.

Corresponding author: Mónica Preciado. E-mail: mpreciado@ubu.es

P. M. Bravo: pmbravo@ubu.es

D. Cárdenas: dcardenas@ubu.es

ABSTRACT

The fatigue properties of high-pressure die-casting (HPDC) magnesium alloys AZ91 exhibit a high variability, due primarily to the porosity that is inherent in the injection process. In the 94% of the studied samples, the porosity in which crack nucleation originates, is at the surface or adjacent to the surface. The threshold stress intensity factor amplitude and the limit of fatigue have been calculated following the classical models of parameterization of defects. A new set of samples were prepared by machining the surface slightly, in order to conserve the microstructure, and the fatigue behavior at low level of stress was improved. All samples were produced in molds with the final shape by HPDC process, which allowed a realistic study of the surface effect and the influence of grain size variation from the edge to the center of the samples.

1. Introduction

Magnesium alloys are increasingly utilized due to their combination of properties including low density, high specific strength, and good castability, which make them the lightest metals available for use in applications, such as automobile equipment, aerospace components, computers, mobile phones and household equipment. One of the more developed magnesium alloys is AZ91, which has exhibited a great potential for use in these applications.

The high-pressure die-casting (HPDC) method is the preferred manufacturing process for the Mg-alloy components used in automotive and numerous other applications. This is due to its advantages like faster prototyping and better casting dimensional accuracy [1] on one hand and on the other because of the benefits involving the high speed production that can be achieved. For several structural automotive applications, fatigue resistance is of prime concern; therefore, it is of interest to understand the effect of microstructure and microstructural defects on the fatigue behavior of HDPC Mg-alloys. The variability in the properties of HDPC materials is a consequence of the strong dependence on the resulting microstructure and the discontinuities produced by the process. To produce components for long life behavior, it is necessary to establish the mechanisms of fatigue and to link the sources of variability with the microstructural features and the different discontinuities present in the material.

Microporosity (on the order of microns) is one of the major problems associated with the HPDC process. Wang et al. [2] made a quantitative study of the gas level in different castings trying to reduce them. Micropores form during the solidification of these alloys primarily due to dissolved gases and shrinkage. Other defects can be due to processing defects such as inclusions, hot-cracks and the presence of an oxide skin. Buffiere et al. [3] reported that pores and voids are generated by dissolved hydrogen during the solidification of the molten alloy, resulting in micro shrinkage and the

formation of artificial gas pores, but also, it was found [4] that the amount of gas introduced to the alloy during processing has no significant influence on the volume fraction of the gas pores. More recently, Li et al. [1] showed that the presence of externally solidified crystals in HPDC magnesium alloys could lead to shrinkage during solidification turning into the formation of porosities. Nevertheless, microporosity impairs the mechanical properties such as ultimate strength, yield strength, ductility and fatigue resistance. It was observed by Eisenmeier et al. [5], from experiments on cyclic deformation of AZ91 alloy, that crack initiation during fatigue cracking occurs in concentration cavities that depend on the porosity levels. The fatigue life in porous magnesium alloys has been studied and Rettberg et al. [6] concluded that the pore size and the pore location were more decisive for AZ91 than for AM60 at low strain amplitudes. Although it is clear that the porosity level significantly influences the fatigue strength, there has been an improvement in the level of porosity compared to the first injected products. Nowadays there is absence of defects like circular shrinkage cavities or big central isolated pores as the ones found by Miriam et al. [7]. In this research, the pores that lead to final fracture have been tried to be identified in order to locate and measure them.

The characterization of HPDC magnesium alloys and the influence of porosity on the fatigue of materials could be performed with samples taken from sheets of different widths with subsequent machining. This method may be unrealistic in terms of the distribution of porosity, defects or the absence of surface finishing effect. The major impact of the surface on the results was stated by some authors [8].

In this work, samples were directly fabricated using the same process followed in real production, thereby reproducing the defects and their distribution encountered in real materials in the form of test coupons. This approach allowed the detailed study of the

microstructure and defects and some modelling theories were used to characterize the fatigue behavior of the HPDC AZ91D alloys. Throughout the investigation, the influence of the superficial pores on the results was observed; as a result, the fatigue behavior of the machined samples was studied by removing 0.3mm from the surface to verify the improvement of the fatigue results for low strength levels under this new condition. This machining operation slow down the high productivity of HPDC process but for simple geometries might be an option. Actually two techniques are used when smoothing the surface is required: polishing and trowalising. If these techniques aim to not only make a surface with better appearance but to eliminate surface pores, the fatigue properties of the real pieces can be improved.

2. Experimental methods

The composition of the AZ91D magnesium used for the present study and determined by an Arc Spark Analyzer was (wt-%): Al, 8.83; Be, 0.001; Cu, 0.007; Fe, 0.003; Mn, 0.32; Si, 0.028 and Zn, 0.6. The microstructure of this alloy (Fig. 1) consists of Mg grains decorated with precipitates in the grain boundary that correspond to a divorced eutectic. The details of these precipitates can be observed in Fig. 2, with a clear distinction between $Mg_{17}Al_{12}$ and Mg (the composition was obtained with the diffractometer, XRD, of the SEM).

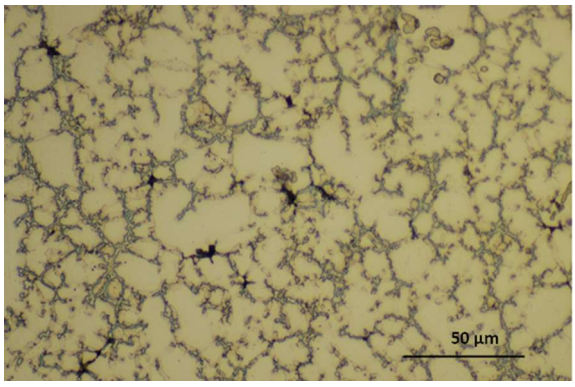

Figure 1. Microstructure of the sample. Grains of Mg with eutectic grain boundaries.

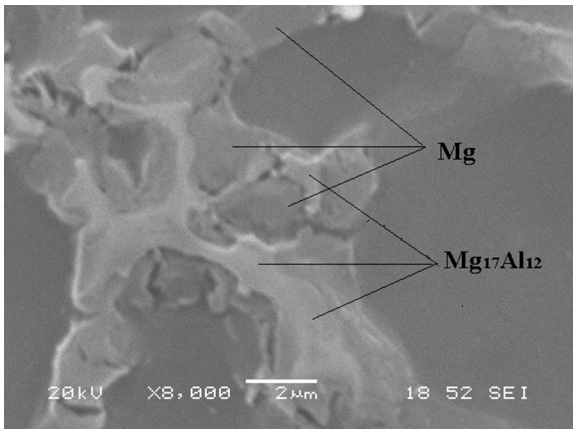

Figure 2. The SEM image of the eutectic: Mg17Al12 – Mg.

There is great variation in the grain size from the center (10 µm) to the sides (5 µm), measured by intercept line technique, as shown in Fig. 3 at low magnification.

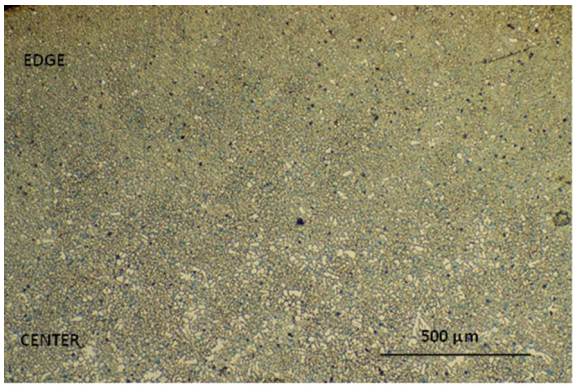

Figure 3. Decrease in grain size from the edge to the center of the samples.

Two sets of fatigue samples were prepared, both with a circular geometry and a diameter of 6.3 mm for the first set of samples and 6 mm diameter after machining for the second set of samples (Fig. 4). In the first set (no machining), the as-cast finish of the specimens was judged to be sufficiently accurate, and only manual grinding to remove excess flash along the parting line of the die was performed.

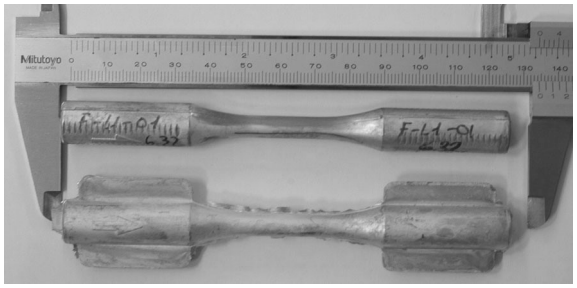

Figure 4. High pressure die casting specimens for fatigue testing.

The fatigue testing was performed in an 810-Material Test System 250 KN, at strength levels of 55%, 60%, 70% 80% and 90% of the yield strength (0.2%), which has a value of 158.2MPa. The stress ratio R was equal to -1, and the frequency of the test was 10Hz. In normal fatigue testing, the strength levels correspond to percentages of the tensile strength, but for HPDC samples, these strength levels are strongly dependent on the elongation and this one is dependent on the porosity (very high in this case) leading to random results that make it difficult to draw reliable conclusions.

2.1.Modelling parameters theories

From the studies of Murakami and Endo [9], when a specimen contains a three-dimensional defect other than a planar crack, the fatigue limit is determined by the threshold condition of the crack emanating from the defect. In this case, the three-dimensional shape of the defect is not directly correlated with the stress intensity factor. Rather, the planar domain (area), which is occupied by projecting the defect onto the plane perpendicular to the maximum principal stress, should be regarded as the equivalent crack, and the stress intensity factor should be evaluated from the equivalent crack.

The stress intensity amplitude is calculated using (for R=-1):

$$K_{max} = \beta\sigma_{max}\{\pi(area)^{1/2}\}^{1/2} \quad (1)$$

β takes a value of 0.65 for surface cracks and 0.5 for internal pores.

The fatigue limit, can be modelled as a function of the $(area)^{1/2}$. From the same author:

$$\sigma_w = \beta(H_v + 120)/\left((area)^{1/2}\right)^{1/6} \quad (2)$$

β takes a value of 1.43 for surface defects and 1.56 for internal pores.

About the stress ratio R, Kujawski and Dinda [10, 11] have contended that a decrease in the stress ratio to a negative magnitude would have no effect on the resulting crack

propagation rate. Their statement was based on the hypothesis that when a crack in a material is subjected to compressive stress, it closes and thus does not grow.

Kazinczy [12] established that the fatigue limit could be expressed by:

$$\sigma_w = \frac{\sigma_{w0}}{1 + K\sqrt{D}} \qquad (3)$$

Where D represents the average size of the defect defined as the diameter of the smallest circle that contains to the defect and σ_{w0} is the fatigue limit of a sample from the same material without defects.

3. Results and Discussion

In the fractographic analysis, two types of initiation points were revealed. The first type corresponds to extreme or nearly extreme pores (Fig. 5), and the second corresponds to large central pores (Fig. 6). Cracks due to fatigue always were initiated in regions of porosity. Most of these porous regions were at the surface (67%) or very near the surface (27%), and only 6% of the porous were in the center.

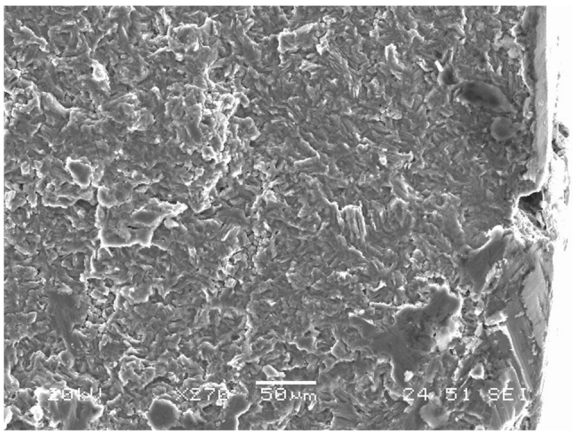

Figure 5. The SEM image of a pore at the surface as the origin of fatigue fracture in the sample.

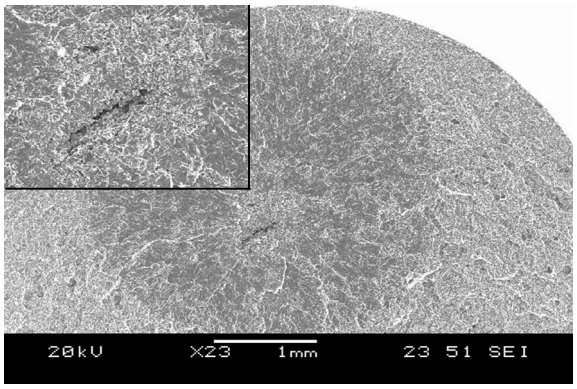

Figure 6. The SEM image of a big pore at the center of the sample as origin of the fatigue fracture.

SEM investigation of the crack initiation served to determine the pores at the crack initiation sites and an image analysis program was used to measure the projected area of the pores. Very small sizes were observed: only 13% of them were larger than 5 x 10^{-3} mm^2, with most of them being approximately 1.2 x 10^{-3} mm^2. As expected, when the pores were in the same zone, larger pore size corresponded to a smaller number of cycles before breakage. In addition, for a high level of strength and similar pores size, the number of cycles until breakage had a low value.

The fact that the majority of the defects that originated the final fracture was located at the edges, leads to the idea that machining the samples to remove part of the porous surface skin could improve the fatigue life by eliminating superficial defects.

At other hand, optical microscopy allowed the observation that the cracks ran across the grain boundaries (Fig. 7). This cracking at the grain boundaries can be explained by the incoherence nature of $Mg_{17}Al_{12}$ with the α-Mg matrix (the magnesium matrix has an hcp lattice whereas the $Mg_{17}Al_{12}$ intermetallic phase has a cubic lattice). It has been stated by Zhai et al. [13] that the twist and tilt angles of the crack plane deflection at the grain boundary are the other key factors that control the path and growth rate of short cracks and could cause the crack to stop. Cavaliere and De Marco [14] noted the increase in the fatigue resistance and the crack growth rate attributed to the enhanced

ductility due to grain refinement. To some degree, the small grain size at the surface counteracts the negative effect of surface defects.

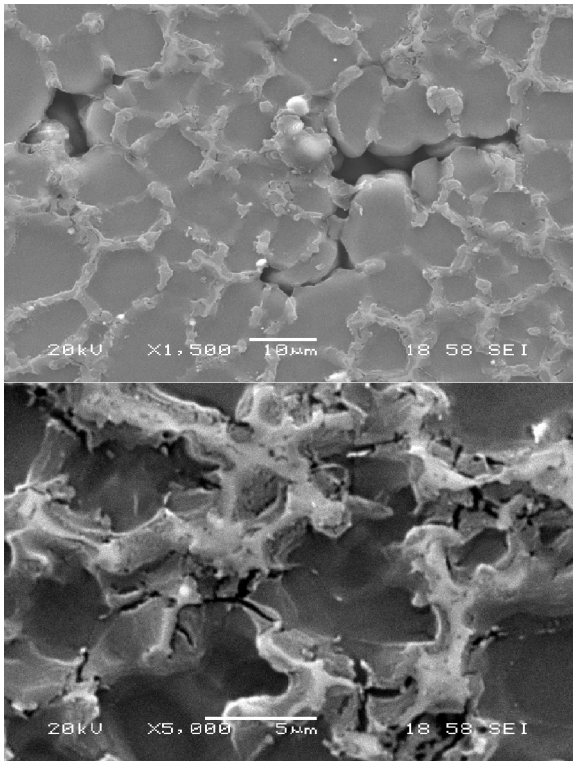

Figure 7. The SEM image of cracking at the grain boundaries.

In the S-N fatigue tests (Fig. 8), the mean fatigue limit of both of the investigated HPDC AZ91 alloy samples has been established as the value below which the specimens did not fail up to 10^7 cycles (the unbroken samples were taken out of the test machine, there is not a number of cycles data). The machined samples showed a better behavior at low strengths; the number of cycles until rupture was almost four times higher than that of the non-machined samples. The fatigue limit for the machined samples was found to be 86.99MPa and for non-machined samples was 79.05MPa. The difference in these values is due to the smaller diameter of the machined samples.

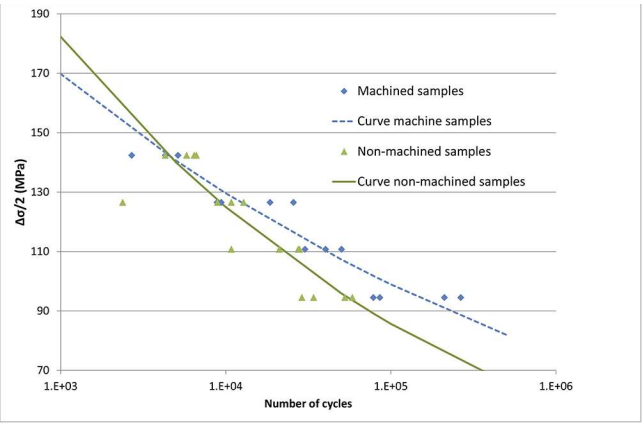

Figure 8. S-N test of the machine and non-machined samples. (The curves are obtained according to the ASTM E739 Standard).

In both sets of samples, the existence of a fatigue limit seems to be due to the lack of propagation of the cracks for low stresses rather than to the lack of conditions that initiate cracking, because the specimens are full of small microcracks that propagate through the grain boundaries.

3.1. Critical stress intensity amplitude

Assuming that one of the pores is the starting points of the crack leading to breakage, and substituting the values of the defect areas (pore areas) into Eq. (1) with their corresponding correction factors and load increments applied, different ΔK_0 values were calculated (Fig. 9). The lowest value corresponds to the threshold value, ΔK_{cr}, of 1.14MPam$^{1/2}$. This value is lower than the other values found by Venkatesman et al. [15] and Horstemeyer et al. [16], of approximately 4MPam$^{1/2}$ and 3.5MPam$^{1/2}$ for the as-obtained samples from die cast specimen, and is slightly higher to the value of 1MPam$^{1/2}$ found by Murugan et al. [17] for samples machined from HPDC pellets, in which there is no large variation in the grain size and for which the surface condition is also different from the surface obtained in real pieces.

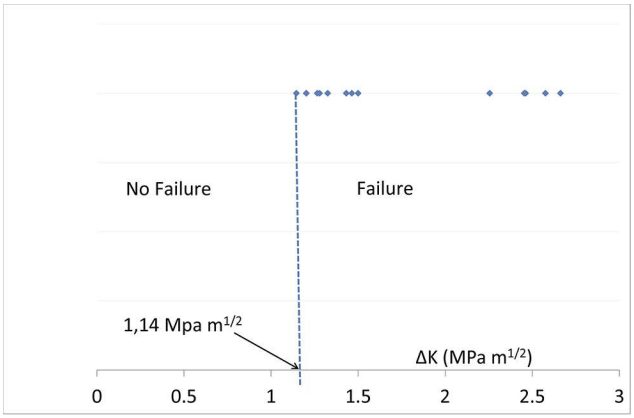

Figure 9. Stress Intensities Factor Amplitude of broken specimens. The vertical line separates the failed and unfailed specimens.

For the machined samples, the SEM analysis indicated that the origin of the cracks was in the edges in only 50% of the cases. The defect size could be clearly observed and measured in three of these samples. In these three cases, the defect was very near the surface but not at the surface (Fig.10). It was not possible to determine a threshold following Murakami´s theories because the area could not be measured in a representative manner. However, it was verified that the defect was always larger than similar defects in the same position of the non-machined samples, and the number of cycles until failure was higher; presumably, the threshold of the critical stress amplitude would have been higher as well.

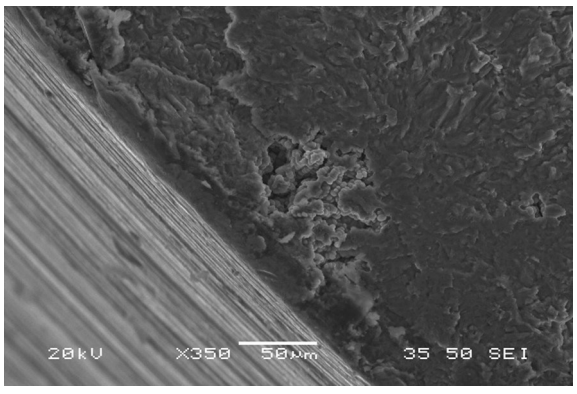

Figure 10. The SEM image of a defect near the surface in a machined sample.

3.2. Fatigue limit

Substituting the value of ΔK_{cr} in Eq. (1) and considering the sizes of the found pores, the value obtained for the fatigue limit was 56.04MPa for the largest porosity and 76.20MPa for the most likely porosity. The value found in the tests was 79.08MPa, very similar to the second calculated value. These results validate the modelling of the default size by the area$^{1/2}$ parameter.

Relating the value of Vickers hardness with the fatigue limit by Eq. (2), the fatigue limit can be obtained; the values of 81.04MPa for the highest porosity and 89.79MPa for the most probable defect size are obtained, similar to the fatigue limit measured in the tests. The model of Kazinczy by applying the Eq. (3) needs the fatigue limit value of a sample free of defects which is impossible because the HPDC process is precisely characterised by the big amount of porosity. Instead, the value 0.5 σ_m of a die cast sample was used, where σ_m was the tensile strength (σ_m= 220MPa). Using the empirical value of the fatigue limit and the diameters of the different pores, a value for K= 0.06 was obtained. Extrapolating this value to the rest of the tests, the average fatigue limit calculated is 73.45MPa. However, it remains to be shown that this value of K is valid for other set of samples and also, defect-free castings cannot be produced in practice, so the value of σ_{w0} is not exact.

4. Conclusions

The real conditions of the HPDC process could be different if the samples are chosen and machined from larger specimens. A study of real finished samples without variations is fundamental in terms of obtaining the grain size distribution that varies from the outer to the inner region of them, as well as the surface conditions and defects due to injection casting.

The Murakami model has been an effective model for HPDC AZ91 alloys in which the area$^{1/2}$ is substituted for the crack length. This model can help to predict ΔK_0 and the fatigue limit.

There are multiple pores in this kind of specimens due to the fabrication process, but superficial pores are, despite the small size, the more determinant in the final fracture.

Light machining of the samples improves the fatigue limit under small loads.

There is evidence of the growth of small cracks originating from microporous regions that follows the grain boundaries. The resistance to crack initiation and propagation may be improved by grain refinement at the surface due to the decreased slip distance with decreasing grain size.

Acknoledgements

This work was supported by the project MAGNO CENIT (2011)

Nomenclature

D = average size of defect, μm

hcp = hexagonal close packed

HPDC = High Pressure Die Casting

Hv = Vickers hardness, Kg/mm^2

K = experimental exponent

K_{max} = maximum stress intensity amplitude, MPa m$^{1/2}$

R = stress ratio

α = phase designation

β = finite correction factor

ΔK_0 = threshold of stress intensity amplitude, MPa m$^{1/2}$

γ = finite correction factor

σ_w = fatigue limit, MPa

σ_{w0} = fatigue limit of a defect-free sample, MPa

References

[1] Li, X., Xiong, S.M., and Guo, Z., 2015, "On the porosity induced by externally solidified crystals in high pressure die-cast of AM60B alloy and its effect on crack initiation and propagation", Mater. Sci. Eng. A, 633, pp. 35-41.

[2] Wang, L., Turnley P., and Savage, G., 2011, "Gas content in high pressure die castings", J Mater. Proc. Tech., 211, pp. 1510-1515.

[3] Buffiere, J. Y., Savelli, S., Jouneau, P. H., Maiere, E., and Fougeres, R., 2001, "Experimental study of porosity & its relation to fatigue mechanisms of model AL-Si7-Mg0.3 cast al alloys", Mater. Sci. Eng. A, 316, pp. 115-26.

[4] Prakash, D. G. L., Prasanna, B., and Regener, D., 2005, "Computational microstructure analyzing technique for quantitative characterization of shrinkage and gas pores in pressure die cast AZ91 magnesium alloys", Comput. Mater. Sci., 32, pp. 480-88.

[5] Eisenmeier, G., Holzwarth, B., Hoppel, H.W., and Mugharbi, H., 2001, "Cyclic deformation and fatigue behaviour of magnesium AZ91", Mater. Sci. Eng. A, 319-321, pp. 578-82.

[6] Rettberg, L. H., Jordon, J. B., Horstemeyer, M. F., and Jones, J. W. 2012, "Low-cycle fatigue behavior of die-casr Mg alloys AZ91 and AM60", Metall. and Mater. Trans. A, 43A, pp. 2260-2274.

[7] Lorenzo, M., Alegre, J. M., and Cuesta, I., 2013, "Magnesium alloy defectology AZ91D high-pressure die cast and influence on the fatigue behavior", Fatigue Fract. Eng. Mater. Struct., 36, pp. 1017-1026.

[8] Korzynski, M., Zarski, T., and Korzynska, K., 2011, "Surface layer condition and the fatigue strength of an AZ91 alloy after ball peening", J Mat. Proc. Tech., 211, pp. 1982-88.

[9] Murakami, Y., and Endo, M., 1992, "The area parameter model for small defects and nonmetallic inclusions in fatigue strength, experimental evidences and applications", In: Proceedings of the theoretical concepts and numerical analysis of fatigue. Birmingham, UK, Warely, Engineering Materials Advisory Services Ltd., Cradley Heath, pp. 51-71.

[10] Kujawski, D., 2001, "A new (KmaxΔK+)0.5 Driving force parameter for crack growth in aluminum alloys", Int. J Fatigue, 23, pp. 733–40.

[11] Dinda, S., Kujawski, D., 2004, "Correlation and prediction of fatigue crack growth for different R-ratios using Kmax and ΔK parameters", Eng. Fract. Mech., 71, pp. 1779–90.

[12] Kazinczy, F., 1970, “Effect of small defects on the fatigue properties of medium strength cast steel”, J. Iron Steel Inst., 208, pp. 851-55.

[13] Zhai, T., Wilkinson, A.J., and Martin, J.W., 2000, “A crystallographic mechanism for fatigue crack propagation through grain boundaries”, Acta Mater., 48, pp. 4917-27.

[14] Cavaliere, P., and De Marco, P., 2007, “Fatigue behaviour of friction stir processed AZ91 magnesium alloy produced by high pressure die casting”, Mater. Charact., 58, pp. 226-32.

[15] Venkateswaran, P., Ganesh, S., Pathak, S. D., Miyashita, Y., and Mutoh, Y., 2004, “Fatigue crack growth behaviour of a die-cast magnesium alloy AZ91D”, Material Lett., 58, pp. 2525-29.

[16] Horstemeyer, M. F., Yang, N., Gall, K., McDowell, D. L., Fan, J., and Gullet, P. M., 2004, “High cycle fatigue of a die cast AZ91E-T4 magnesium alloy”, Acta Mater., 52, pp. 1327-36.

[17] Murugan, G., Raghukandan, K., Pillai, U.T.S., and Mahadevan, K., 2009, “High cyclic fatigue characteristics of gravity cast AZ91 magnesium alloy subjected to transverse load”, Mater. Des., 30, pp. 2636-41.

Figure Captions

Figure 1. Microstructure of the sample. Grains of Mg with eutectic grain boundaries.

Figure 2. The SEM image of the eutectic: $Mg_{17}Al_{12}$ – Mg.

Figure 3. Decrease in grain size from the edge to the center of the samples.

Figure 4. High pressure die casting specimens for fatigue testing.

Figure 5. The SEM image of a pore at the surface as the origin of fatigue fracture in the sample.

Figure 6. The SEM image of a big pore at the center of the sample as origin of the fatigue fracture.

Figure 7. The SEM image of cracking at the grain boundaries.

Figure 8. S-N test of the machine and non-machined samples. (The curves are obtained according to the ASTM E739 Standard).

Figure 9. Stress Intensities Factor Amplitude of broken specimens. The vertical line separates the failed and unfailed specimens.

Figure 10. The SEM image of a defect near the surface in a machined sample.